XXI ENMC
ENCONTRO NACIONAL DE MODELAGEM COMPUTACIONAL
IX ECTM
ENCONTRO DE CIÊNCIA E TECNOLOGIA DE MATERIAIS

08 a 11 de Outubro de 2018
Instituto Federal Fluminense
Búzios - RJ

A NEW TWO-COMPONENT RED BLOOD CELL MODELLING APPROACH

Luca Meacci[1] - luca.meacci@usp.br
Gustavo C. Buscaglia[1] - gustavo.buscaglia@icmc.usp.br
Roberto F. Ausas[1] - rfausas@icmc.usp.br
Fernando Mut[2] - fmut@gmu.edu
[1]Instituto de Ciências Matemáticas e de Computação, Universidade de São Paulo - São Carlos, SP, Brazil
[2]Bioengineering Department, George Mason University - Fairfax, Virginia, USA

Abstract. *This work consists in the presentation of a computational model to study normal and pathological behavior of red blood cells in slow transient processes that can not be accompanied by pure particle methods (the required time steps are very small). The basic model, inspired by the best models currently available, considers the cytoskeleton as a discrete non-linear elastic structure. The novelty of the proposed work, which will extend the simulation times and the robustness of the code, is to couple this skeleton with continuum models instead of the more common discrete models (molecular dynamics, particle methods) of the lipid membrane. The interaction of the solid cytoskeleton with the membrane, which is a two-dimensional fluid, will be done through adhesion forces adapting efficient solid-solid adhesion algorithms. The continuous treatment of the fluid parts is well justified by scale arguments and leads to much more stable and precise numerical problems when, as is the case, the size of the molecules* ($0.3nm$) *is much smaller than the overall size* ($\simeq 8000nm$)

Keywords: *Red blood cell, Cytoskeleton, Lipid bilayer, Ahesion problem, Modeling of biological systems*

INTRODUCTION

The whole volume of RBCs inside de human circolatory system constitues around the $35-50\%$ of the blood's one. This means that the peculiar characterists of the RBC highly affects the byological funtion of the blood delivering oxygen. Ulker et al. (2009) in a recent study have also shown that the exposure of RBCs to physiological shear stress allows the synthesis of the nitric oxide enzymatically, contribuiting so to the regulation of vascular tonus. Moreover, the hig concentration in the blood of RBCs has direct consequence in the haemodynamics (Popel & Johnson, 2005) (Mchedlishvili & Maeda, 2001).

In the human body an erythrocyte consists in a biocave disk shape, flattened and depressen in the middle, with a cross section of dumbbell shape (Li-Guo et al., 2010). In an undeformed

state, its diameter is $6 - 8\mu\,m$ on the circular discoid plane and the thickness on the bIn consequence, tiocave radial plane has an average value of $2\mu\,m$. The average volume of a RBC is $90\mu\,m^3$ and the surface area of about $136\mu\,m^2$ (Ju et al., 2015). While in blood vessels with a diameter larger than $200\mu\,m$ (like the arteries) we can neglet the size effect of the RBCs and model the blood as a homogenneus non-Newtonian fluid, on the other hand, when we consider the circulation inside vessels with smaller diameter (arterioles, venules and capillares), i.e. when the vessel's internal diameter is comparable with the size of the RBCs, to consider the suspension and the morphological evolution of the erytrocite becomes pivotal. In this second case, the RBC can pass through small capillares whose inner diameter are smaller then the cells ones, inducing the cell to change its shape form the bioncave original one to a bullet or a paracadute (for then recover its initial shape). It is therefore fundamental, in order to understand the blood flow and its functions in microcirculation, to face up to the modeling of a RBC. Usually, in the life-science research, bulk methods for sumilation considering million of cells are normally performed for studying the cell behavoiur because they are simple, avalaible and well estabilisched (Svahn & Berg, 2007). However cells in a similar environment can show heterogeneous behaviour within a population and potentially significant cellular behaviour may not be captured by bulk techniques (Bao et al., 2014). De facto, single-cell studies are important for understanding higher-level systemsm such as tissues and organisms, and for developing therapeutic approaches (Carlo & Lee, 2006). This work aims to contribute within the single-cell studies.

A RBC is a nucleus-free cell that basically consists of a fluid-like lipid bilayer contributing to the bending resistance and an attached spectrin network (cytoskeleton) that helps maintain cell shape during motion. Transmembrane proteins connect the lipid bilayer and spectrin components. The current state of the art is that models must account for each of two components separately to accurately mimic the physics of the RBC. A computational model that separately accounts for each component has recently proved useful in the analysis of healthy and diseased RBCs (Li et al., 2014; Chang et al., 2017). The network submodel consists of junctions (nodes) that are joined by springs that obey a worm-like-chain nonlinear law. The lipid bilayer submodel consists of a surface of Dissipative-Particle-Dynamics (DPD) particles endowed with bending energy, elastic and viscous interactions, and thermal fluctuations. The cytoskeleton-bilayer interaction in the aforementioned model consists of a short-range force between the nodes of the network and the bilayer particles. This force is attractive in the direction normal to the bilayer surface, and viscous-friction-like in the tangential one. DPD is a particle-based method, quite similar to coarse grained molecular dynamics, in that each particle represents a molecule or a group of molecules. When the number of molecules is very large continuum models are more accurate and efficient than particle-based models. The typical length of a spectrin filament is about 70 nm, leading to about 10^5 edges in an actual RBC cytoskeleton. The typical number of lipid molecules in the bilayer of an RBC, on the other hand, is about 700 million.

In our new RBC modelling approach, we propose a new two-component model in which the cytoskeleton is kept discrete as before, but the lipid bilayer is modeled as a continuous surface fluid. In particular, we adopt the viscous liquid-shell model with Canham-Helfrich bending energy described by Arroyo (2010). Its discretization follow that of Rodrigues et al. (2015), which is the first one with sufficient generality to accomplish this task. The two components are coupled by adhesion forces that mimic the attachment of the cytoskeleton nodes to the bilayer integral proteins.

MATHEMATICAL FORMULATION

We can consider a red blood cell as a mechanical system that, from the kinematical point of view, has a configuration described by the state $\mathcal{X}$ of the cytoskeleton and the state $\mathcal{Y}$ of the membrane. In Figure 1 we show a scheme of a RBC depicting the two components of the model. The configuration $\mathcal{X}$ represents a state of the cytoskeleton, which in our model is a set of N_X balls of radius R representing the junctional complexes of the cytoskeleton. In this way, appropriate coordinates for $\mathcal{X}$ are the positions of the *nodes* of the cytoskeleton model, which are the centers of the aforementioned balls. These coordinates will be denoted by $\{\boldsymbol{X}^j\}_{j=1}^{N_X}$.

Figure 1- Skecth of the problem.

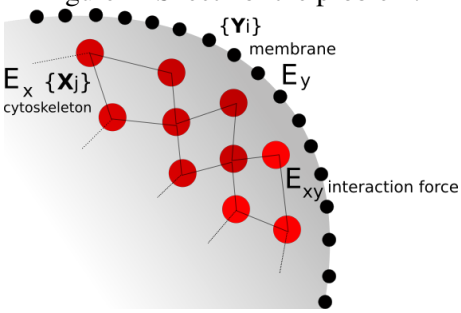

Similarly, $\mathcal{Y}$ is a configuration of the lipid membrane, which in the exact problem is an element of an infinite-dimensional manifold of possible membrane shapes. For numerical purposes, however, it is always modeled as a finite-dimensional manifold spanned by generalized coordinates. In our case we adopt parameterizations that are defined by the positions of N_Y points, the *nodes* of the membrane model. The coordinates of any configuration $\mathcal{Y}$ are thus $\{\boldsymbol{Y}^i\}_{i=1}^{N_Y}$. From these coordinates the *geometrical position* of the membrane,

$$\Gamma(\mathcal{Y}) = \{\boldsymbol{y} \in \mathbb{R}^3 \mid \boldsymbol{y} \text{ belongs to the membrane surface } \}\,, \tag{1}$$

can be reconstructed.

The energy of the proposed two-component system $\mathcal{E}$ (that clearly depends on $\mathcal{X}$ and $\mathcal{Y}$) is decomposed into the sum

$$\mathcal{E}(\mathcal{X},\mathcal{Y}) = \mathcal{E}_X(\mathcal{X}) + \mathcal{E}_Y(\mathcal{Y}) + \mathcal{E}_{XY}(\mathcal{X},\mathcal{Y}) \tag{2}$$

where $\mathcal{E}_X$ is the intrinsic skeleton energy, $\mathcal{E}_Y$ the intrinsic membrane energy, and $\mathcal{E}_{XY}$ the interaction energy between the cysoskeleton and the membrane.

Consequently, the instantaneous motion of the cytoskeleton is described by rates of change of $\mathcal{X}$, which can formally be expressed as

$$\mathcal{U} = \frac{d\mathcal{X}}{dt}\,, \tag{3}$$

which in practice means that the velocity of the cytoskeleton nodes obeys

$$\boldsymbol{U}^j = \frac{d\boldsymbol{X}^j}{dt}\,. \tag{4}$$

The instantaneous motion of the membrane particles, on the other side, is characterized by the rates of change of $\mathcal{Y}$, as follow

$$\mathcal{W} = \frac{d\mathcal{Y}}{dt}\,. \tag{5}$$

This means that the tracking of the surface is *Lagrangian*. In particular, in the discrete case, the velocity of the i-th membrane node,

$$\boldsymbol{W}^i = \frac{d\boldsymbol{Y}^i}{dt}\,, \tag{6}$$

coincides with that of the lipid particle at $\boldsymbol{Y}^i(t)$. In this latter sentence "lipid particle" is to be understood not as a lipid molecule but as a small but macroscopic chunk of lipid material, in the spirit of Continuum Mechanics.

We consider as starting point for the mathematical formulation of the problem the **principle of virtual work** demanding that in our case the work done by the energies yet defined for an admissible virtual variation the configuration variables and the work done by the dissipative forces is ugual to the work done by the external forces of the system (Lanczos, 1970). The corresponding expression can be formally written as

$$\begin{aligned} d_X\mathcal{E}(\mathcal{X},\mathcal{Y}) \bullet \delta\,\mathcal{X} + d_Y\mathcal{E}(\mathcal{X},\mathcal{Y}) \bullet \delta\,\mathcal{Y} + \mathcal{D}(\mathcal{X},\mathcal{Y},\mathcal{U},\mathcal{W}) \bullet (\delta\,\mathcal{X},\delta\,\mathcal{Y}) \;= \\ = \mathcal{F}_X \bullet \delta\,\mathcal{X} + \mathcal{F}_Y \bullet \delta\,\mathcal{Y} \end{aligned} \tag{7}$$

where

- $d_X\mathcal{E}(\mathcal{X},\mathcal{Y}) \bullet \delta\,\mathcal{X}$ is the infinitesimal change $\delta\mathcal{E}$, when the state of the system is perturbed from $(\mathcal{X},\mathcal{Y})$ to $(\mathcal{X}+\delta\,\mathcal{X},\mathcal{Y})$,
- the bullet $\bullet$ is an appropriate duality product which will detailed later,
- $d_Y\mathcal{E}(\mathcal{X},\mathcal{Y}) \bullet \delta\,\mathcal{Y}$ is the infinitesimal change $\delta\mathcal{E}$, when the state of the system is perturbed from $(\mathcal{X},\mathcal{Y})$ to $(\mathcal{X},\mathcal{Y}+\delta\,\mathcal{Y})$,
- $\mathcal{D}(\mathcal{X},\mathcal{Y},\mathcal{U},\mathcal{W}) \bullet (\delta\,\mathcal{X},\delta\,\mathcal{Y})$ is the dissipation of the system (i.e., the work of its internal dissipative forces), when the system is perturbed by $(\delta\mathcal{X},\delta\mathcal{Y})$, and,
- the right-hand side is the virtual work of external forces.

Explicit expressions for the several terms in (7) can be derived by the mathematical modeling of each of the two components (bilayer, cytoskeleton) of the system, and of their interaction, as brifly presented described below.

Lipid bilayer model

Being Γ the average surface of the bilayer at time t, we define $\mathbf{u}$ and σ as the velocity and the surface tension of the bilayer respectively. Also let H be an *average curvature* of Γ, $\check{\mathbf{n}}$ the normal vector and $\boldsymbol{\kappa}$ the *mean curvature vector*, defined as $\boldsymbol{\kappa} = H\,\check{\mathbf{n}}$. We also need the tangential projector $\mathbb{P} = \mathbb{I} - \check{\mathbf{n}} \otimes \check{\mathbf{n}}$. The *tangential gradient* ∇_Γ is the operator defined as $\nabla_\Gamma f = \mathbb{P}\,\nabla\widehat{f}$, where $f : \Gamma \to \mathbb{R}$ is any function and $\widehat{f}$ an arbitrary extension of f to an open neighborhood of $\Gamma \subset \mathbb{R}^3$.

In the currently available model the interaction with the inner and outer fluid is simplified. The only force the fluid exerted on the bilayer comes from a pressure difference uniform p.

With these definitions, the viscous dynamics of the bilayer lipidic (Scriven, 1960; Rahimi % Arroyo, 2012), considering the energy of bending, is given by the unique fields $\mathbf{u}$, σ, $\boldsymbol{\kappa}$ and the only scalar $p \in \mathbb{R}$ such that

$$\int_\Gamma 2\,\mu\, D_\Gamma \mathbf{u} : D_\Gamma \mathbf{v} \; - p \int_\Gamma \mathbf{v}\cdot\check{\mathbf{n}} \; + \; \int_\Gamma \sigma\, \nabla_\Gamma \cdot \mathbf{v} \; +$$

$$+c_{\text{CH}} \int_\Gamma \left[(\mathbb{I} - 2\,\mathbb{P}) \nabla_\Gamma \boldsymbol{\kappa} : \nabla_\Gamma \mathbf{v} + \frac{1}{2} (\nabla_\Gamma \cdot \boldsymbol{\kappa})\, (\nabla_\Gamma \cdot \mathbf{v}) \right] \;\; = \;\; \int_\Gamma \mathbf{f}^\Gamma \cdot \mathbf{v} \tag{8}$$

$$\int_\Gamma \xi\, \nabla_\Gamma \cdot \mathbf{u} \;\; = \;\; 0 \tag{9}$$

$$\int_\Gamma \boldsymbol{\kappa} \cdot \boldsymbol{\zeta} \;\; = \;\; \int_\Gamma \mathbb{P} : \nabla_\Gamma \boldsymbol{\zeta} \tag{10}$$

$$\int_\Gamma \mathbf{u} \cdot \check{\mathbf{n}} \;\; = \;\; 0 \tag{11}$$

$\forall\, (\mathbf{v}, \xi, \boldsymbol{\zeta}) \;\in\; \mathbf{V} \times Q \times \mathbf{K}$, where $\mathbf{V}$ and $\mathbf{K}$ are essencially $(H^1(\Gamma))^3$ and $Q = L^2(\Gamma)$. The surface viscosity is denoted by μ and the forces field $\mathbf{f}^\Gamma : \Gamma \to \mathbb{R}^3$ includes all the forces derived from the interaction with the cytoskeleton and external interactions. The term containing the constant c_{CH} comes from the energy of Canham-Helfrich (Canham, 1970; Helfrich, 1973; Seguin & Fried, 2014), i.e.,

$$\mathcal{E}_{\text{bend}} = \frac{c_{\text{CH}}}{2} \int_\Gamma H^2 \; = \frac{c_{\text{CH}}}{2} \int_\Gamma \|\boldsymbol{\kappa}\|^2 \,. \tag{12}$$

The methodology to solve this part of the bi-component model arises by the discretization of the above variational formulation in space and in time. This has already been developed and was recently published (Rodrigues et al., 2015). It incorporates automatic adjustment of the time step and surface remeshing (Löhner, 1996). The theoretical framework comes from the works by Dziuk, Elliot, and others (Bonito et al., 2010; Dziuk & Elliott, 2006; Dziuk & Elliott, 2013; Rusu, 2005).

In this new approach we incorporate the interaction with the cyto-skeleton, as the the model described below.

Cytoskeleton model

The cytoskeleton will be treated by trying to follow the nature of its components, basically a spectrin fiber special joints (Gratzer, 1981). The mesh is considered as a set of nodes (junctions) joined by molecular chains that are usually represented by Worm-Like-Chains (Hansen et al., 1996; Fedosov et al., 2010; Fedosov et al., 2011).

The typical length of a spectrin filament is 70 nm, leading to about 10^5 edges in a real erythrocyte cyto-skeleton. This number, however large, is numerically treatable and also there are coarse-grained models that can be applied to save computing effort (Pivkin & Karniadakis, 2008). This is very different for the lipid bilayer, in which the number of particles (phospholipids) is approximately 700 million. The novelty of the project consists of taking advantage of the continuum limit for the lipid bilayer, keeping the cyto-skeleton discrete.

The elastic energy spectrin mesh is described by

$$V = \sum_j \left[\frac{k_B T \ell_m \,(3x_j^2 - 2x_j^3)}{4p(1 - x_j)} + \frac{k_p}{(n-1)\ell_j^{n-1}} \right] \tag{13}$$

where ℓ_j is the filament length j, ell_m is the maximum extension of these filaments, $x_j = ell_j/\ ell_m$, p is the length of persistence, k_BT is the unit of energy and n and k_p parameters. This results in a macroscopic shear modulus (for an hexagonal cell) of (see (Fedosov et al., 2011))

$$G_0 = \frac{\sqrt{3}\,k_BT}{4p\ell_m x_0}\left(\frac{x_0}{2(1-x_0)^3} - \frac{1}{4(1-x_0)^2} + \frac{1}{4}\right) + \frac{\sqrt{3}k_p(n+1)}{4\,\ell_0^{n+1}} \tag{14}$$

with ℓ_0 is the equilibrium spacing and $x_0 = \ell_0/\ell_m$.

The integration of the cytoskeleton equations will be carried out using classical techniques of computational solids mechanics.

Interaction Model

The interaction between the bilayer and the cytoskeleton will be modeled as adhesion of soft bodies, adapting the formulation of Sauer (2012) based on the models and available data (Freund & Lin, 2004; Kuusela & Wolfgang, 2009, Pajic-Lijakovic & Milivojevic, 2014; Peng et al., 2013). If denoting by Υ *the adherent surface* of the cytoskeleton, the contact energy takes the general form

$$\mathcal{E}_{\text{con}} = \int_\Gamma \int_\Upsilon \beta_\Gamma\ \beta_\Upsilon\ \phi(\|\mathbf{x}^\Gamma - \mathbf{x}^\Upsilon\|)\ d\mathbf{x}^\Gamma\ d\mathbf{x}^\Upsilon \tag{15}$$

where ϕ is the potential of interaction (in Joule/m^4) and β_Γ, β_Υ are dimensionless scalars. The forces resulting from this energy are calculated considering $\delta\mathbf{x}^\Gamma$ and $\delta\mathbf{x}^\Upsilon$ in the positions of the bilayer and the particles of the cytoskeleton:

$$\begin{aligned}
\delta\mathcal{E}_{\text{con}} &= \int_\Gamma\int_\Upsilon \beta_\Gamma\beta_\Upsilon\phi'(\|\mathbf{x}^\Gamma - \mathbf{x}^\Upsilon\|)\,\frac{\mathbf{x}^\Gamma - \mathbf{x}^\Upsilon}{\|\mathbf{x}^\Gamma - \mathbf{x}^\Upsilon\|}\cdot\left(\delta\mathbf{x}^\Gamma - \delta\mathbf{x}^\Upsilon\right)\,d\mathbf{x}^\Gamma\,d\mathbf{x}^\Upsilon &(16)\\
&= -\int_\Gamma \mathbf{f}^{\text{con},\Gamma}(\mathbf{x}^\Gamma)\cdot\delta\mathbf{x}^\Gamma\,d\mathbf{x}^\Gamma - \int_\Upsilon \mathbf{f}^{\text{con},\Upsilon}(\mathbf{x}^\Upsilon)\cdot\delta\mathbf{x}^\Upsilon\,d\mathbf{x}^\Gamma &(17)
\end{aligned}$$

where $\mathbf{f}^{\text{con},\Gamma}(\mathbf{x}^\Gamma)$ is the net force in $\mathbf{x}\Gamma$ produced by interaction with the *whole* Υ,

$$\mathbf{f}^{\text{con},\Gamma}(\mathbf{x}^\Gamma) = -\,\beta_\Gamma\int_\Upsilon \beta_\Upsilon\phi'(\|\mathbf{x}^\Gamma - \mathbf{x}^\Upsilon\|)\,\frac{\mathbf{x}^\Gamma - \mathbf{x}^\Upsilon}{\|\mathbf{x}^\Gamma - \mathbf{x}^\Upsilon\|}\,d\mathbf{x}^\Upsilon\ . \tag{18}$$

Replacing Γ with Υ we obtain $\mathbf{f}^{\text{con},\Upsilon}(\mathbf{x}^\Upsilon)$. Keeping $\delta\mathbf{x}^\Gamma = \delta\mathbf{x}^\Upsilon$ constant, it follows that $\int_\Gamma \mathbf{f}^{\text{con},\Gamma} + \int_\Upsilon \mathbf{f}^{\text{con},\Upsilon} = 0$, as expected.

SIMULATIONS

We present in this section the simulation of a relaxation process, i.e. starting from a initial configuration and in absense of external forces we allow the system to goes to the equilibrium state.

We set a cytoskeleton with 313 nodes and we discretized the bilayer with 4500 nodes. For the time discretization we adopted a fixed time step $\Delta\,t = 10^{-5}$. The setup of parameters is reported in Table 1.

Table 1- Setup of parameters.

Value	Symbol	Description	Model
1.0	$k_B\,T$	Energy unit	(WLC)
-18.0	k_p	POW constant	(WLC)
-0.08928	p	Persistent length	(WLC)
0.625	ℓ_0	Edge initial length	(WLC)
2	n	POW exponent	(WLC)
1.0	β_Γ	Bilayer interaction constant	(INT)
1.0	β_Υ	Cyto interaction constant	(INT)
6	k	Coefficient Lennard-Jones potential	(INT)
0.125	R	Radius of cyto-sphere	(INT)
1.0	μ	Viscosity	(BIL)
20.0	C_H	Canham constant	(BIL)
79.6	V_0	Initial RBC volume	(BIL)

In Figure 2 we display a certain time evolution step of the lipidic bilayer and the magnitude of the curvature. It is plotted also a section of the RBC showing the finite element mesh used. In the same Figure (below) we report the same results but now including the the cytoskeleton into the model. The section of the RBC allows to see the cytoskeleton network. It is interesting to see that the presence of the cytoskelton affects the evolution in terms of distribution of nodes of the bilayer and of the curvature. Finally, in Figures 3 and 4, we also show the time evolution of some relevant global quantities, namely, the bending energy, the internal pressure, the area and enclosed volume for both cases. We can appreciate the influence of the cytoskeleton over the bilayer comparing the bilayer energy with and without the cytoskeleton attached to it. We also note some jumps in the area and volume (that are essentially constants). These jumps are due to the re-meshing process used to keep the mesh distortion under control.

CONCLUSIONS

In this work we have presented a new approach for modeling a single RBC. According to this, we have motivated the need of a new two-component model for a sigle RBC. We have coupled to the consolidate worm-like-chain approach for the cytoskeleton a continuum model for the lipid bilayer, based on a viscous liquid-shell model with Canham-Helfrich bending energy. An original contribution is presented by the introduction of the adhesion forces for reproducing the attachment of the cytoskeleton nodes to the bilayer integral proteins. We tested the two-component RBC modelling approach on a simple example of relaxation of the cell.

Understanding better the behaviour of a red blood cell means to give a strong contribution to the comprehension of life. Thanks to modern technology, the accuracy of mathematical models can be proven by experimental laboratory tests. *Vice versa*, mathematical modeling can help to identify the reasons behind what is physically observed. Our next step is to adapt the code in order to simulate the fundamental experiments of micropipette aspiration and optical tweezing. Our deliverable is a software for the “in silico” (or virtual) simulation of RBCs that extends the range of spatial and temporal scales of current simulators as the OpenRBC code (Tang et al., 2017) and the implementation in LAMMPS of Fu et al. (2017).

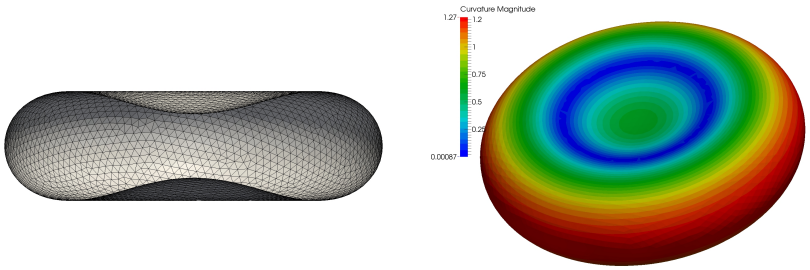

Lipidic bilayer negleting cytoskeleton and interaction forces.

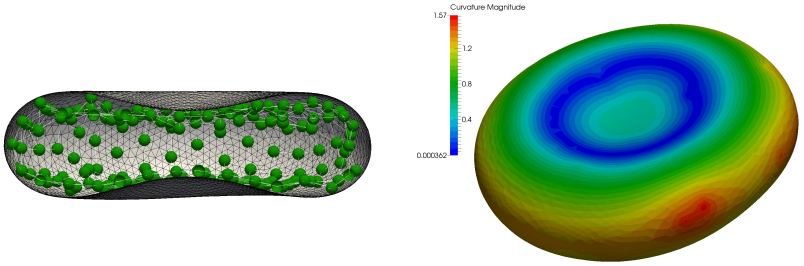

Lipidic bilayer considering cytoskeleton and interaction forces.

Figure 2- Screenshots of the simulation of the evolution of the RBC in the relaxation process ($t = 0.15$).

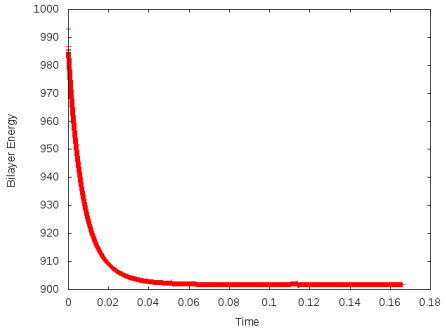

Bilayer energy.

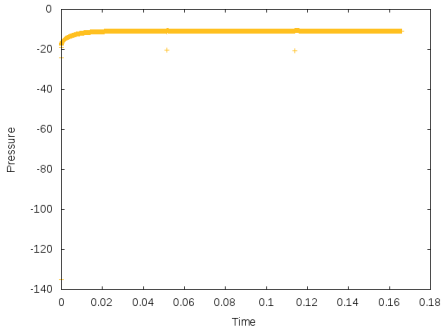

Pressure.

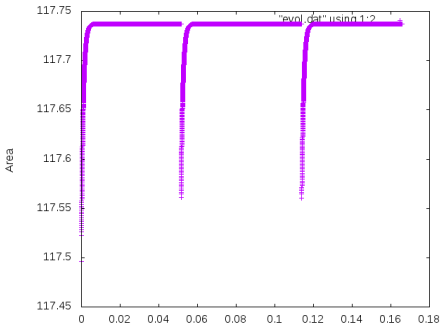

Area.

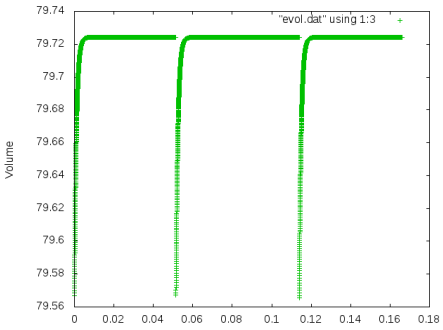

Volume.

Figure 3- Simulation of the time evolution of the lipidic bilayer (without cytoskeleton).

Acknowledgements

Luca Meacci acknowledges with appreciation the foudation CAPES (Coordenação de Aperfeiçoamento de Pessoal de Nível Superior) of the Ministry of Education of Federal Republic of Brazil for

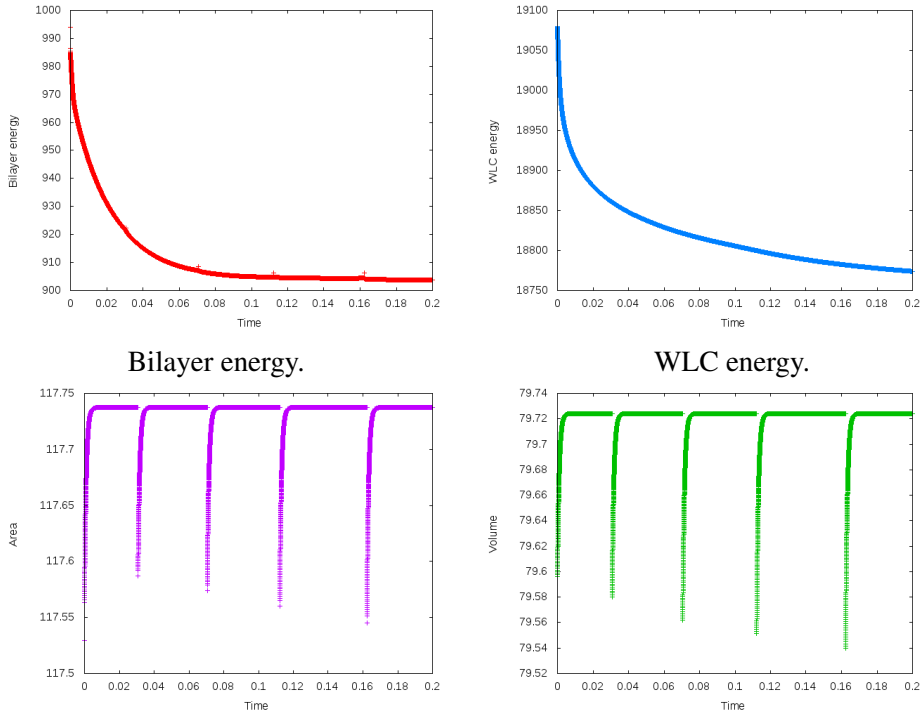

Bilayer energy. WLC energy.

Area. Volume.

Figure 4- Simulation of the time evolution of the full two-component model (lipidic bilayer with cytoskeleton and interaction forces).

receiving economic support within the funding program of academic excellence PROEX (Programa de Excelência Acadêmica).

REFERENCES

Arroyo, M., DeSimone, A., Heltai, L. (2010). The role of membrane viscosity in the dynamics of fluid membranes. arXiv preprint arXiv:1007.4934.

Bonito, A., Nochetto, R. H., Pauletti M. S. (2010), Parametric FEM for geometric biomembranes. J. Comput. Phys., 229(9):3171–3188.

Bao, G., Bazilevs, Y., Chung, J.H., Decuzzi, P., Espinosa, H. D., Ferrari, M., Gao, H., Hossain, S. S., Hughes, T. J., Kamm, R. D. et al. (2014), Usnctam perspectives on mechanics in medicine. Journal of The Royal Society Interface, The Royal Society, v. 11, n. 97, p. 20140301.

Canham, P. (1970), The minimum energy of bending as a possible explanation of the biconcave shape of the human red blood cell. J. Theor. Biol., 26(1):61–81.

Carlo, D. D. & Lee, L. P. (2006), Dynamic single-cell analysis for quantitative biology. [S.l.]: ACS Publications.

Chang, H. Y., Li, X., Li, H., Karniadakis, G. E. (2016). MD/DPD multiscale framework for predicting morphology and stresses of red blood cells in health and disease. PLoS computational biology, 12(10), e1005173.

Dziuk, G., Elliott, C. M. (2006). Finite elements on evolving surfaces. IMA J. Numer. Anal., 27:262–292.

Dziuk, G., Elliott, C. M. (2013). Finite element methods for surface PDEs. Acta Numer., 22:289–396.

Fedosov, D., Caswell B., Karniadakis, G. (2010), A multiscale red blood cell model with accurate mechanics, rheology and dynamics. Biophys. J., 98:2215– 2225.

Fedosov, D., Lei, H., Caswell, B., Suresh, S., Karniadakis, G. (2011), Multiscale modeling of red blood cell mechanics and blood flow in malaria. PLoS Comput. Biol., 7:e1002270.

Freund, L., Lin, Y. (2004), The role of binder mobility in spontaneous adhesive contact and implications for cell adhesion. J. Mech. Phys. Solids, 52:2455–2472.

Fu, S. P., Peng, Z., Yuan, H., Kfoury, R., Young, Y. N. (2017). Lennard-Jones type pair-potential method for coarse-grained lipid bilayer membrane simulations in LAMMPS. Computer Physics Communications, 210, 193-203.

Gratzer, W. (1981), The red cell membrane and its cytoskeleton. Biochem. J., 198:1–8.

Hansen, J., Skalak, R., Chien, S., Hoger, A. (1996). An elastic network model based on the structure of the red blood cell membrane skeleton. Biophys. J., 70:146–166.

Helfrich, W. (1973). Elastic properties of lipid bilayers – theory and possible experiments. Z. Naturforsch. C, 28:693–703.

Lanczos, C. (1970). The variational principles of mechanics, 4th edn. [S.l.]: Toronto University Press, Toronto.

Li, X., Peng, Z., Lei, H., Dao, M., Karniadakis, G. E. (2014). Probing red blood cell mechanics, rheology and dynamics with a two-component multi-scale model. Phil. Trans. R. Soc. A, 372(2021), 20130389.

Li-Guo, J., Heng-An, W., Xiao-Zhou, Z., Xiu-Xi, W. (2010), Coarse-grained molecular dynamics simulation of a red blood cell. Chinese Physics Letters, IOP Publishing, v. 27, n. 2, p. 028704.

Löhner, R. (1996), Regridding surface triangulations. J. Comput. Phys., 126(1):1–10.

Mchedlishvili, G., Maeda, N. (2001), Blood flow structure related to red cell flow: determinant of blood fluidity in narrow microvessels. The Japanese journal of physiology, Physiological Society of Japan, v. 51, n. 1, p. 19–30.

Ju, M.; Ye, S. S.; Namgung, B.; Cho, S.; Low, H. T.; Leo, H. L.; Kim, S. (2015). A review of numerical methods for red blood cell flow simulation. Computer methods in biomechanics and biomedical engineering, Taylor & Francis, v. 18, n. 2, p. 130–140.

Kuusela, E., Wolfgang, A. (2009). Continuum model of cell adhesion and mi- gration. J. Math. Biol., 58(1-2):135–161.

Pajic-Lijakovic, I., Milivojevic, M. (2014), Modeling analysis of the lipid bilayer-cytoskeleton coupling in erythrocyte membrane. Biomech. Model. Mechano-biol., 13:1097–1104.

Peng, Z., Li, X., Pivkin, I., Dao, M., Karniadakis, G., Suresh, S. (2013), Lipid bilayer and cytoskeletal interactions in a red blood cell. Proc. Natl. Acad. Sci. USA, 110(33):13356–13361.

Pivkin, I., Karniadakis, G. (2008), Accurate coarse-grained modeling of red blood cells. Phys. Rev. Lett., 101:118105.

Popel, A. S., Johnson, P. C. (2005), Microcirculation and hemorheology. Annu. Rev. Fluid Mech., Annual Reviews, v. 37, p. 43–69.

Rodrigues, D. S., Ausas, R. F., Mut, F., Buscaglia, G. C. (2015). A semi-implicit finite element method for viscous lipid membranes. Journal of Computational Physics, 298, 565-584.

Rahimi, M., Arroyo, M. (2012), Shape dynamics, lipid hydrodynamics, and the complex viscoelasticity of bilayer membranes. Phys. Rev. E, 86(1):011932, Jul 2012.

Rusu, R. (2005), An algorithm for the elastic flow of surfaces. Interf. Free Bound., 7:229–239.

Sauer, R. (2012), Computational contact formulations for soft body adhesion. In Advances in soft matter Mechanics. Springer.

Scriven, L. (1960). Dynamics of a fluid interface: Equations of motion for Newtonian surface fluids. Chem. Eng. Sci., 12:98–108.

Seguin, B., Fried, E. (2014), Microphysical derivation of the Canham-Helfrich free-energy density. J. Math. Biol., 68(3):647–665.

Svahn, H. A. & Berg, A. van den (2007). Single cells or large populations? Lab on a Chip, Royal Society of Chemistry, v. 7, n. 5, p. 544–546.

Tang, Y. H., Lu, L., Li, H., Evangelinos, C., Grinberg, L., Sachdeva, V., Karniadakis, G. E. (2017). OpenRBC: a fast simulator of red blood cells at protein resolution. Biophysical journal, 112(10), 2030-2037.

Ulker, P., Sati, L., Celik-Ozenci, C., Meiselman, H., Baskurt, O. (2009), Mechanical stimulation of nitric oxide synthesizing mechanisms in erythrocytes. Biorheology, IOS Press, v. 46, n. 2, p. 121–132.